Reconstitution of Experimental Neurogenic Bladder Dysfunction Using Skeletal Muscle-Derived Multipotent Stem Cells

Article *in* Transplantation · February 2010

Impact Factor: 3.83 · DOI: 10.1097/TP.0b013e3181d45a7f · Source: PubMed

9 authors, including:

Tetsuro Tamaki
Tokai University School of Medicine, Ise…
62 PUBLICATIONS **1,353** CITATIONS
SEE PROFILE

Akio Hoshi
Tokai University
41 PUBLICATIONS **354** CITATIONS
SEE PROFILE

Reconstitution of Experimental Neurogenic Bladder Dysfunction Using Skeletal Muscle-Derived Multipotent Stem Cells

Masahiro Nitta,[1,2] Tetsuro Tamaki,[2,4] Kayoko Tono,[2] Yoshinori Okada,[2,3] Maki Masuda,[2] Akira Akatsuka,[2,3] Akio Hoshi,[1,2] Yukio Usui,[1] and Toshiro Terachi[1]

Background. Postoperative neurogenic bladder dysfunction is a major complication of radical hysterectomy for cervical cancer and is mainly caused by unavoidable damage to the bladder branch of the pelvic plexus (BBPP) associated with colateral blood vessels. Thus, we attempted to reconstitute disrupted BBPP and blood vessels using skeletal muscle-derived multipotent stem cells that show synchronized reconstitution capacity of vascular, muscular, and peripheral nervous systems.

Methods. Under pentobarbital anesthesia, intravesical pressure by electrical stimulation of BBPP was measured as bladder function. The distal portion of BBPP with blood vessels was then cut unilaterally (experimental neurogenic bladder model). Measurements were performed before, immediately after, and at 4 weeks after transplantation as functional recovery. Stem cells were obtained from the right soleus and gastrocnemius muscles after enzymatic digestion and cell sorting as $CD34^+/45^-$ (Sk-34) and $CD34^-/45^-$ (Sk-DN). Suspended cells were autografted around the damaged region, whereas medium alone and $CD45^+$ cells were transplanted as control groups. To determine the morphological contribution of the transplanted cells, stem cells obtained from green fluorescent protein transgenic mouse muscles were transplanted into a nude rat model and were examined by immunohistochemistry and immunoelectron microscopy.

Results. At 4 weeks after surgery, the transplantation group showed significantly higher functional recovery (~80%) than the two controls (~28% and 24%). The transplanted cells showed an incorporation into the damaged peripheral nerves and blood vessels after differentiation into Schwann cells, perineurial cells, vascular smooth muscle cells, pericytes, and fibroblasts around the bladder.

Conclusion. Transplantation of multipotent Sk-34 and Sk-DN cells is potentially useful for the reconstitution of damaged BBPP.

Keywords: Radical hysterectomy, Pelvic plexus, Intravesical pressure.

(*Transplantation* 2010;89: 1043–1049)

Postoperative neurogenic bladder dysfunction, such as sensory loss and storing and voiding dysfunctions, is a major complication after radical hysterectomy for cervical cancer (*1*). Autonomic nerve supply for the bladder is mainly derived from the bladder branch of the pelvic plexus (BBPP), which is formed by the hypogastric, pelvic splanchnic, and somatic nerves. The BBPP plays a vital role in the coordinated contraction of the smooth muscles of the bladder and the bowel. Bladder dysfunction during radical hysterectomy is considered to be caused by accidental or unavoidable disruption of these innervating autonomic nerve fibers and blood vessels to the bladder (*2*, *3*). Generally, the incidence of postoperative neurogenic bladder dysfunction is reported to be 70% to 85% in patients who have received radical hysterectomy (*1*, *4*). It has also been reported that bladder function gradually recovers during the postoperative follow-up period; however, more than 50% of women with normal urinary tract function preoperatively require abdominal straining to void, even at 6 months postsurgery (*4*). Thus, numerous pa-

This work was supported by Tokai University Research aid.

[1] Department of Urology, Division of Surgery, Tokai University School of Medicine, Shimokasuya, Isehara, Kanagawa 259-1143, Japan.
[2] Muscle Physiology and Cell Biology Unit, Department of Regenerative Medicine, Division of Basic Clinical Science, Tokai University School of Medicine, Shimokasuya, Isehara, Kanagawa 259-1143, Japan.
[3] Teaching and Research Support Center, Tokai University School of Medicine, Shimokasuya, Isehara, Kanagawa 259-1143, Japan.
[4] Address correspondence to: Tetsuro Tamaki, Ph.D., Muscle Physiology and Cell Biology Unit, Department of Regenerative Medicine, Division of Basic Clinical Science, Tokai University School of Medicine, 143 Shimokasuya, Isehara, Kanagawa 259-1143, Japan.

M.N. worked as first author and participated in the writing of the paper; T.T. participated in research design, the writing of the paper, and data analysis; K.T. participated in data analysis; Y.O. participated in data analysis; M.M. participated in data analysis; A.A. participated in conducting the research (immunoelectron microscopy) and data analysis; A.H. participated in data analysis; Y.U. participated in data analysis; T.T. participated in research design.

E-mail: tamaki@is.icc.u-tokai.ac.jp

Received 25 December 2009. Revision requested 25 December 2009.
Accepted 7 January 2010.

ISSN 0041-1337/10/8909-1043
DOI: 10.1097/TP.0b013e3181d45a7f

tients are affected by these dysfunctions and desired to achieve early and complete recovery.

Surgical procedures have recently been modified to preserve these nerves (*5*–*7*). Todo et al. (*5*) reported that in the case of nerve-sparing radical hysterectomy, there have been no patients complaining of urinary difficulty at 12 months after surgery although urodynamic studies have revealed the presence of underlying bladder dysfunction (incomplete recovery). However, there are several issues with nerve-sparing radical hysterectomy. If the tumor has invaded tissues around the spared autonomic nerves, it is difficult (wholly impossible) to use nerve-sparing techniques (*6*) although experienced surgeons may still be able to carry out the procedure (*7*). Therefore, simpler methods to treat bladder dysfunction after radical hysterectomy are necessary.

The main cause of bladder dysfunction after radical hysterectomy is considered to be the disruption of BBPP and colateral blood vessels; thus, if reconstitution of peripheral BBPP nerves and their blood vessels can be achieved, significant results are expected. In this context, we previously identified two stem cell populations in the interstitial spaces of murine skeletal muscle (*8*, *9*). Cells in the $CD34^+/CD45^-$ fraction (Sk-34 cells) and $CD34^-/CD45^-$ fraction (Sk-DN cells) are able to synchronously reconstitute nerve-muscle-blood vessel units after transplantation into severely damaged skeletal muscle with significant functional recovery through cellular differentiation into skeletal muscle cells, vascular cells (vascular smooth muscle cells, pericytes, and endothelial cells), and peripheral nervous cells (Schwann cells and perineurium) (*10*, *11*). Recently, these cells were applied to the reconstitution of severely damaged urethral sphincter with disruption of supplied nerves and blood vessels and significantly contributed to both morphological and functional recovery (*12*).

Therefore, the purpose of this study was to examine whether the transplantation of skeletal muscle-derived multipotent stem cells is able to facilitate reconstitution of damaged BBPP associated with blood vessels and to achieve early and fundamental recovery of neurogenic bladder dysfunction. For this purpose, we developed a rat experimental neurogenic bladder model and its functional measurement by electrical stimulation through BBPP. Autologous transplantation was used for functional recovery analysis as simulation of an actual human therapy, and heterologous transplantation (green fluorescence transgenic mouse to nude rat) was used to determine morphological reconstitution.

MATERIALS AND METHODS

Animals

Female wild-type Sprague-Dawley rats (age, 8–12 weeks; weight, 180±20 g) were used in the autologous transplantation experiment. In this experiment, the soleus and gastrocnemius muscles of the right leg were removed and prepared for stem cell isolation. For heterologous (mouse to nude rat) transplantation, green fluorescence protein transgenic mice (GFP-Tg mice; C57BL/6 TgN[act EGFP]Osb Y01; provided by Okabe (*13*), Osaka University, Osaka, Japan; age, 4–8 weeks) were used as donor animals, and female athymic nude rats (F344/NJcl-mu/rnu; CLEA, Tokyo, Japan) were used as recipient animals. All experimental procedures were conducted in accordance with the Japan Physiological Society Guidelines for the Care and Use of Laboratory Animals, as approved by Tokai University School of Medicine Committee on Animal Care and Use.

Cell Purification

Skeletal muscle-derived multipotent stem cells were extracted from the thigh and lower leg muscles (tibialis anterior, extensor digitorum longus, soleus, plantaris, gastrocnemius, and quadriceps femoris) of GFP-Tg mice and the soleus and gastrocnemius muscles of rats (for autograft experiment), as described previously (*8*). Whole nonminced muscles were treated with 0.1% collagenase type IA (Sigma-Aldrich, Tokyo, Japan) in Dulbecco's modified Eagle's medium (DMEM) containing 5% to 10% fetal calf serum with gentle agitation for 2 hr at 37°C. Extracted cells were filtered through 70-, 40-, and 20-μm nylon strainers to remove muscle fibers and other debris, followed by washing and resuspension in Iscove's modified Dulbecco's medium containing 10% fetal calf serum, thus, yielding enzymatically extracted cells. Extracted mouse cells were stained with allophycocyanin-conjugated anti-mouse CD34 (RAM34, 17–0341; eBioscience, San Diego, CA) and pacific blue-conjugated anti-mouse CD45 (30-F11, 103126; BioLegend, San Diego, CA). Sk-34 ($CD34^+/CD45^-$), Sk-DN ($CD34^-/CD45^-$), and $CD45^+$ cells were then collected. Extracted rat cells were stained with anti-rat CD45 (OX-1, PharMingen, San Diego, CA) and anti-rat CD34 (AF4117; R&D Systems, Minneapolis, MN). Live cells were counted after cells showing positive for propidium iodide (dead cells) were excluded. Cell analysis and sorting were carried out on a FACSAria (Becton Dickinson Japan, Tokyo, Japan).

Experimental Neurogenic Bladder Model and Functional Measurement

Surgical procedures and functional measurements were performed under pentobarbital anesthesia (40 mg/kg, intraperitoneal). Under pentobarbital anesthesia, an intravesical catheter (3-Fr tube, 49B87, ATOM Disposable Indwelling Tube; ATOM, Tokyo, Japan) was inserted into the dome of the bladder through urethra. Animals were fixed in the supine position, and the bladder and BBPP were exposed through a lower midline abdominal incision. Custom-made Ag/Ag bipolar electrodes (inter electrode distance, 4 mm) were then placed under the right side of the BBPP (Fig. 1A). Bladder function was measured as a variant of intravesical pressure by electrical stimulation from BBPP. Intravesical catheter was connected to the pressure transducer (DT-XX; Becton Dickinson, Sparks, MD). Approximately 0.5 mL of 0.01 M phosphate-buffered saline (PBS) was injected into the emptied bladder through the intravesical catheter to maintain initial baseline pressure. The transducer was connected to an amplifier (AP-621G; Nihon Kohden, Tokyo, Japan), and pressure changes were recorded on a Linearcorder (Mark VII, WR3101; Graphtec, Tokyo, Japan). Square pulses (4 V, 1 ms pulse, 20 Hz, and 5 s) were delivered through a stimulator (Digital Stimulator ME-6012; MEC, Tokyo, Japan). Stimulation was applied three times in a single measurement and averaged (mean±SE mm H_2O). After the first measurement (preoperative [pre-OP] value), BBPP associated with blood vessels was unilaterally cut with forceps at distal from the electrode (small distance from the bladder; Fig. 1B) in the experimental neurogenic bladder model. At this time, the surface of the bladder wall adhering to BBPP was also damaged and exfoliated with blood vessels. After 20 min, stimulation was repeated and intravesical pressure was recorded in the same manner as above (immediately after operation [IA-OP] value). Electrodes were then removed and direct stem cell transplantation around the damaged BBPP area was performed (see below). At 4 weeks after cell transplantation, bladder function was measured in the same manner as measured for pre-OP and IA-OP (4 weeks after OP value; Fig. 2).

Cell Transplantation

We performed two types of cell transplantation: autologous and heterologous. In autologous cell transplantation, the right lower hind limb soleus and gastrocnemius muscles were removed from Sprague-Dawley rats before the measurement of bladder function, according to the method for the compensatory muscle hypertrophy model (*14*–*16*). Then, Sk-34 and Sk-DN cells were obtained from these muscles. In this compensatory hypertrophy model, the remaining plantaris muscle worked as plantar flexor with sufficient muscle enlargement after chronic stretch stimulation, and thus, the rats were able to move freely in their cages. After functional measurement (see above), a cocktail of freshly sorted Sk-34+Sk-DN cells was suspended in 10 μL of

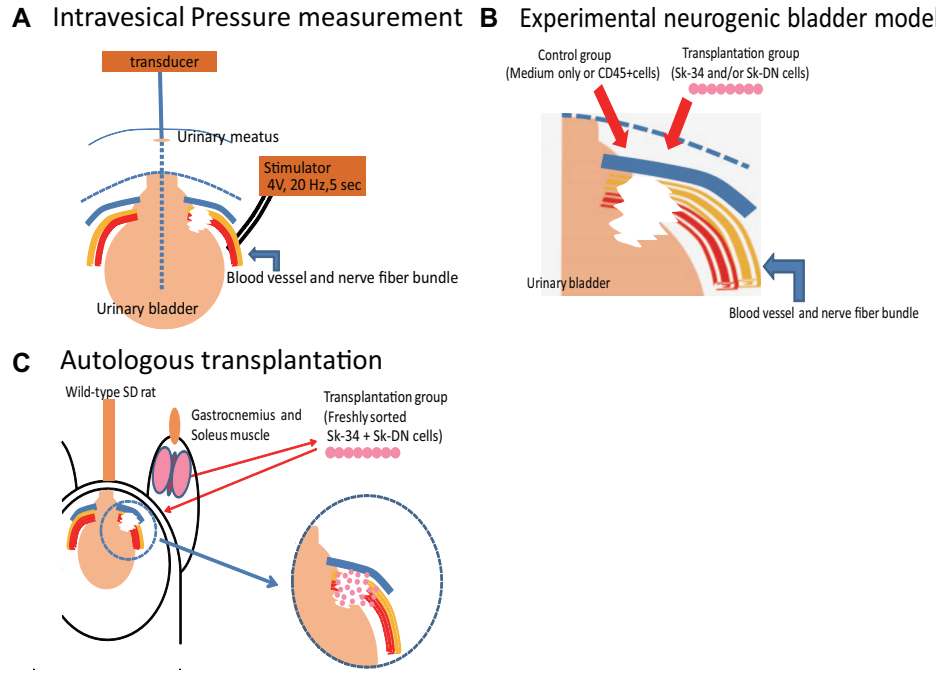

FIGURE 1. Schematic illustration of measurement of intravesical pressure (A), experimental neurogenic bladder model (B), and autologous transplantation using freshly sorted Sk-34+ Sk-DN cells, obtained from the right lower hind limb soleus and gastrocnemius muscles (C). This experiment was a functional recovery analysis. Bladder branch of the pelvic plexus (BBPP) and concomitant blood vessels were manually damaged, and skeletal muscle-derived stem cells were transplanted around the damaged region. Intravesical pressure induced by electrical stimulation from the proximal portion of BBPP was measured through an intravesical catheter connected to a pressure transducer.

DMEM and directly transplanted around the damaged BBPP. The same amount of DMEM solution with $CD45^+$ cells (control 2) or without any cells (control 1) was applied to the two control groups. This experiment was performed for analysis of functional reconstitution. In this functional analysis, mixed Sk-34+Sk-DN cells were used for the autograft experiment and longitudinal analysis in the same individuals; thus, cell transplantation was performed once.

On the other hand, in heterologous cell transplantation, for the purpose of morphological analysis, both Sk-34 and Sk-DN cells were obtained from GFP-Tg mouse muscles. In this analysis, both types of cells were separately transplanted to independently determine the morphological contribution of each cell fraction and whether there were differences, in contrast to functional analysis, in which mixed Sk-34+Sk-DN cells were used. Sk-34 cells were transplanted in a freshly sorted state. Sk-DN cells were cultured for 5 days and expanded because the number of cells in the Sk-DN fraction was small when compared with Sk-34 cells (1:16–20), at initial isolation (*10*, *11*, *17*). Sk-DN cells were cultured in a collagen-based clonal cell culture system (Collagencult H4741; StemCell Tech., Vancouver, Canada) with 10 ng/mL basic fibroblast growth factor and 20 ng/mL epidermal growth factor, which allows a high colony formation rate (>40%) and typical sphere formation (*10*, *11*, *17*). $CD45^+$ cells were also sorted and used as controls for histological analysis in cell transplantation experiments. Each cell fraction was suspended in 10 μL of DMEM ($5–7\times10^5$ cells) and directly scattered around the damaged portion using a micropipette (Fig. 1C). This experiment was carried out for morphological, immunohistochemical, and immunoelectron microscopic analysis. In both functional and morphological experiments, the fibrin sealant (Beriplast; ZLB Behring, Melbourne, Australia) was used to coat the damaged area to reduce additional bleeding and to prevent the diffusion of the transplanted cells.

Macroscopic Observation

At 4 weeks after surgery, macroscopic analysis was performed under a fluorescence dissection microscope (SZX12; Olympus, Tokyo, Japan). Nude rats were given an overdose of pentobarbital (60 mg/kg, intraperitoneal), a lower abdominal midline incision was made to expose the bladder, and the cell implantation region was observed and photographed through a GFP filter.

Immunostaining and Immunoelectron Microscopy

For immunostaining and immunoelectron microscopic analysis, recipient nude rats were perfused with warm 0.01 M PBS through the abdominal aorta, followed by fixing with 4% paraformaldehyde/0.1 M phosphate buffer after macroscopic observation (see above). The bladder was removed and postfixed overnight with 4% paraformaldehyde/0.1 M phosphate buffer at 4°C and was then washed with a graded sucrose (0%–25%)/0.01 M PBS series, embedded in optimum compound (O.C.T compound; Tissue-Tek, Sakura Finetechnical Co., Ltd., Tokyo, Japan), and frozen at −80°C. Subsequently, several 7-μm sections were obtained. Localization of nerve fibers (axons) was detected by mouse anti-Neurofilament 200 monoclonal antibody (N-200; dilution, 1:7000; incubation, room temperature for 1 hr; Sigma, St. Louis, MO), and the blood vessels were detected with mouse anti-α-smooth muscle actin (αSMA Cy3-conjugated; 1:1500; room temperature for 1 hr; Sigma) monoclonal antibody. Reactions were visualized using Alexa Fluor-594-conjugated goat anti-mouse antibodies (1:500; room temperature for 2 hr; Molecular Probes, Eugene, OR). For immunoelectron microscopy, sections were stained with anti-GFP polyclonal antibody (Molecular Probes) and anti-rabbit IgG horseradish peroxidase-conjugated secondary antibody (1:200; 4°C overnight; Dako, Carpinteria, CA). Reactions were visualized with 3,3-diaminobenzidine (DAB) after fixation in 1% glutaraldehyde/0.1 M phosphate buffer. Sections were then fixed in 1% osmium tetroxide/0.05 M phosphate buffer and prepared for electron microscopic analysis. Details of immunoelectron microscopy were as described previously (*8*, *10*, *11*, *17*).

RESULTS

Functional Assessment of Reconstituted Bladder

Typical raw data on intravesical pressures are shown in Figure 2A. At pre-OP, intravesical pressure rose in response to each electrical stimuli; however, no pressure changes were detected at IA-OP (after distally cutting BBPP). This indicates that the applied stimulations were correctly conducted along BBPP and did not defuse into surrounding tissue, and that the distal cutting of BBPP was correctly performed. At 4 weeks after OP, intravesical pressure rose slightly in the control group, but apparent increases in pressure response were observed in the transplantation group. Mean intravesical pressure at pre-OP was 7.9 ± 1.1 cm H_2O in control 1, 8.8 ± 1.1 cm H_2O in control 2, and 9.7 ± 1.1 cmH_2O in the transplantation group. These pre-OP (intact) values were significantly reduced at IA-OP (~0 cm H_2O). At 4 weeks after OP, mean

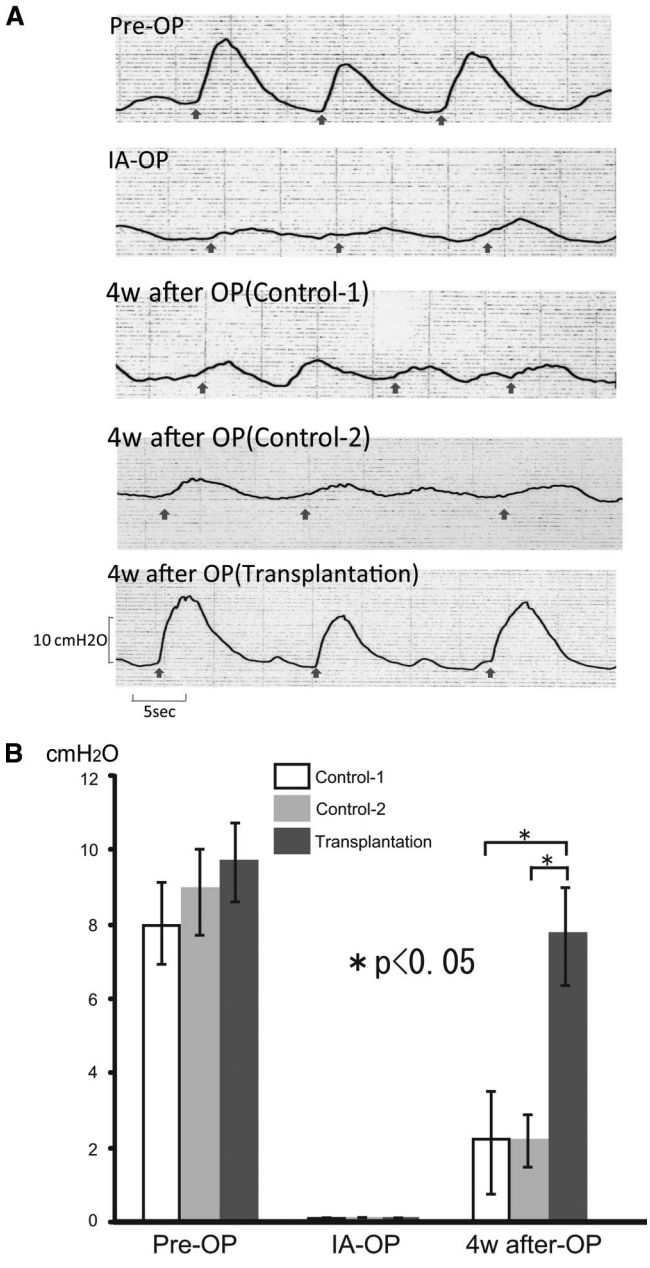

FIGURE 2. Typical low data for intravesical pressure (A) and mean intravesical pressure at preoperative (pre-OP), immediately after operation (IA-OP), and 4 weeks after OP (B). The transplantation group showed significant recovery (~80%), whereas controls showed only ~28% and 24% recovery at 4 weeks after OP. Control 1; medium only (non-cell transplantation); control 2; $CD45^+$ cell transplantation; transplantation; Sk-34+Sk-DN cell transplantation.

intravesical pressure was 2.2±1.6 cm H_2O (n=7) in control 1, 2.1±0.3 cm H_2O (n=4) in control 2, and 7.6±1.4 cm H_2O (n=8) in the transplantation group. When these data were compared with the recovery ratio versus pre-OP values in each group, the transplantation group showed significantly greater recovery (78.4%, $P<0.05$), whereas the control groups showed 27.8% (control 1) and 23.9% (control 2) recoveries (Fig. 2B). These data clearly indicate that transplanted Sk-34+Sk-DN cells significantly contributed to functional recovery of the damaged BBPP and blood vessel bundle.

Macroscopic and Microscopic Observation of BBPP and Blood Vessels

To determine overall macroscopic tissue regeneration, the damaged BBPP, blood vessels, and the surrounding region in the GFP^+-cell transplanted recipient nude rats were analyzed using a fluorescence dissection microscope. Numerous GFP^+ tissues were seen around the bladder neck (Fig. 3A). In addition, GFP^+ nerve-like tissues, probably regenerated nerves, extended on the recipient bladder surface (arrows in Fig. 3B). Donor cell-derived GFP^+ cells and tissues were also detected outside of the bladder muscle layer on histological sections (Fig. 3C), thus suggesting reconstitution of the damaged bladder surface after removal of adherent blood vessels. There was no GFP^+ cells and tissues detected after $CD45^+$ cell transplantation (data not shown).

Immunohistochemical Detection of Donor-Derived Blood Vessels and Nerve Fiber-Related Cells

Engrafted donor cells were then examined by immunohistochemical analysis. Nerve fibers and blood vessels were detected using anti-N-200 and anti-α-SMA. Nerve bundles included anti-N-200-positive nerve fibers (red reactions) around the bladder, and these were associated with GFP^+ reactions, some of which were close to nerve fibers, possibly

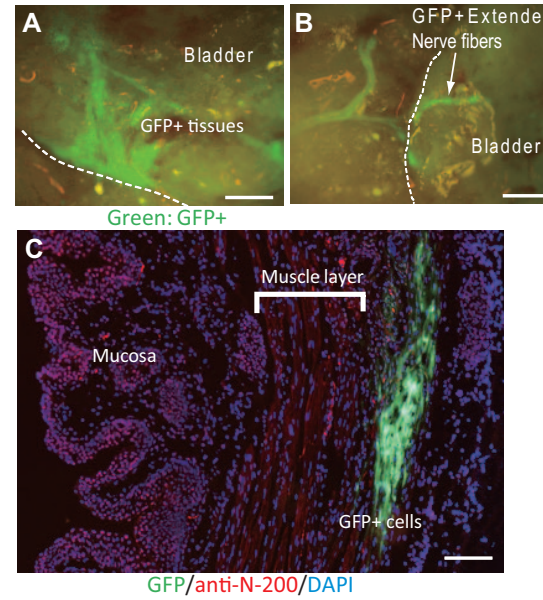

FIGURE 3. Fluorescence macroscopic view (A and B) and histological profile (C) of transplanted nude rats. Donor cell-derived green fluorescence $protein^+$ (GFP^+) tissues are observed on the bladder surface (A). GFP^+ nerve-like tissue, probably extended nerve fibers can be seen around the bladder (B). On the cross-section, a large number of GFP^+ tissues were seen outside of the bladder smooth muscle layer (C). Photographs A and C from Sk-34 cell transplantation group; B from Sk-DN transplantation group. Green = GFP, red = N-200, and blue = DAPI. Scale bars are 1 mm in A and B and are 100 μm in C.

due to cross-reactions (red+green=yellow reactions; arrows in Fig. 4A) but actually did not (refer to legend of Fig. 5). Similarly, GFP$^+$ cells and tissues (arrowheads in Fig. 4B) were evident in the surrounding area of vascular smooth muscle layer as positive for anti-α-SMA (red reactions). In Figure 4C, GFP$^+$ cells were also observed in the blood vessel wall showing positive for anti-α-SMA, and some GFP$^+$ cells were anti-α-SMA$^+$; these were probably vascular smooth muscle cells (arrows in Fig. 4C). There were no GFP$^+$ cells seen on histological sections in the CD45$^+$ cell transplantation group (data not shown).

Immunoelectron Microscopic Detection of Donor-Derived Vascular and Neural Cells

To further confirm the detailed contributions of the transplanted donor cells to blood vessels and nerve fibers, we performed immunoelectron microscopy using anti-GFP and DAB reaction products. Reaction products of DAB (dark dots) were detected around nonmyelinated nerve fiber axons (arrows in Fig. 5A and B), and Schwann cells were clearly seen (SW; B, higher magnification of region outlined in A). GFP$^+$ perineurium or perineurial (PN) cells surrounding the outer layer of the nonmyelinated nerve bundle was also evident (arrowheads, Fig. 5A). GFP$^+$ Schwann cells associated with multiple axons were evident between recipient bladder smooth muscles (Fig. 5C), whereas donor cell-derived GFP$^+$ fibroblasts (FB in Fig. 5D) were seen adjacent to nonmyelinated nerve fibers associated with GFP$^+$ Schwann cells (arrows in Fig. 5D). GFP$^+$ vascular smooth muscle cells were observed in the conduit blood vessel (Fig. 5E). GFP$^+$ cells indicated by squares in E showed contractile filaments (arrows in Fig. 5F). On the other hand, small capillaries exhibited GFP$^+$ pericyte-like cells situated outside of endothelial cells (arrow in Fig. 5G). These results strongly suggest that skeletal muscle-derived multipotent stem cells differentiate into neural cells (Schwann cells and PN cells), blood vessel-related cells (vascular smooth muscle cells and pericytes), and protein-producing cells (fibroblasts) and suggest a contribution to significant functional recovery. Note that similar trends in immunohistochemistry and immunoelectron microscopy were consistently obtained after Sk-34 and Sk-DN cell transplantation. Thus, there appears to be no differences in morphological reconstitution capacity between Sk-34 and Sk-DN cells.

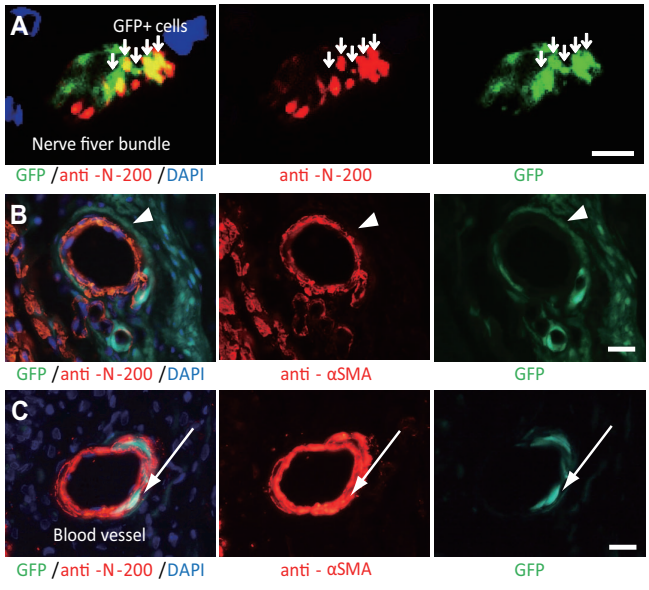

FIGURE 4. Immunohistochemical detection of donor-derived green fluorescence protein$^+$ (GFP$^+$) cells for nerve fibers and blood vessels. (A) Several GFP$^+$ cells (arrows in A) were observed in nerve bundles positive for anti-N-200 (red reactions). (B) Similarly, several GFP$^+$ tissues can be seen around blood vessels positive for anti-α-smooth muscle actin (anti-α-SMA) (red reactions). GFP$^+$ cells surrounded the vascular smooth muscle layer (arrowhead), as if supporting blood vessels. (C) GFP$^+$ cells in conduit blood vessel wall were also positive for α-SMA (arrow, red reactions), indicating vascular smooth muscle cells. Photographs A and C from the Sk-34 cell transplantation group; B from the Sk-DN transplantation group. Scale bars, 10 μm.

DISCUSSION

In this study, we developed an experimental neurogenic bladder model in rats by the blunt ablation of BBPP and associated blood vessels, and we measured the dynamic changes in intravesical pressure through electrical stimulation of BBPP pre- and postablation. A stable increase in intravesical pressure was seen at pre-OP, but a significant reduction in pressure was seen immediately after BBPP ablation (IA-OP; Fig. 2A and B). This indicates that innervation to the bladder was disrupted, similarly to neurogenic bladder in human cases. Kuwabara et al. (*18*) used a similar approach to identify and protect bladder branches of the pelvic nerves during radical hysterectomy in human patients with cervical cancer. Reported raw data on intravesical pressure changes both in human and the present rat model (Fig. 2A) are similar. Therefore, the present rat BBPP damage model may be considered a valid experimental model for neurogenic bladder. In addition, functional data in this study were obtained by longitudinal analysis through the same individuals, even in animal experiments, and morphological contributions of transplanted cells were simultaneously clarified by immunohistochemistry and immunoelectron microscopy using GFP-Tg mice and a nude rat BBPP damage model.

At 4 weeks after surgery, the transplantation group showed a significantly greater functional recovery rate (~80%) than the non-cell transplanted control 1 (~ 28%) and CD45$^+$ cell transplanted control 2 (~24%) groups. This indicates that transplanted multipotent Sk-34 and Sk-DN cells clearly contribute to the functional recovery of experimental neurogenic bladder. Supporting this functional data, GFP$^+$ donor-derived cells were actively implanted around the bladder and surrounding tissues (Fig. 3A) and were found to be incorporated into nerve bundles (Fig. 4A) and blood vessels (Fig. 4B and C) in the damaged BBPP after differentiation into Schwann cells and perineurium (Fig. 5A), vascular smooth muscles, and pericytes (Fig. 5E and G). Reconstituted axons were GFP negative, however, thus suggesting that transplanted Sk-34 and Sk-DN cells reconstituted the outer layer of nerve fibers composed of Schwann and PN cells, and recipient nerve axons extended and reconnected through these reconstituted Schwann cells/perineurium guide cylin-

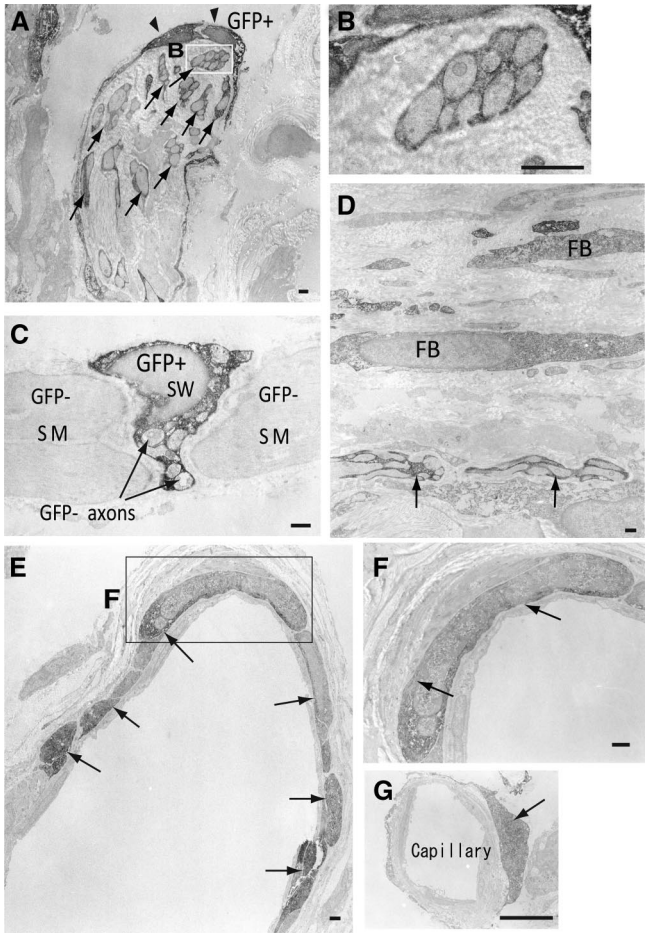

FIGURE 5. Immunoelectron microscopic detection of donor cell-derived neural cells, vascular cells, and fibroblasts. Green fluorescence protein$^+$ (GFP$^+$) donor-derived cells were visualized by 3,3-diaminobenzidine (black dots). (A) GFP$^+$ Schwann cells (arrows in A) adhering to axons in nerve bundles were evident. GFP$^+$ perineurial cells (arrowheads in A) also surround nerve bundles. (B) Higher magnification photograph corresponding to white box in panel (A). GFP$^+$ Schwann cells were clearly observed around non myelinated nerve axons (GFP$^-$). This close localization of nerve axons and Schwann cells may reflect the immunostaining in Figure 4A, represented by yellow reactions (green + red). (C) Several GFP$^-$ nerve axons of small diameter run through between bladder smooth muscles (SM) with GFP$^+$ Schwann (SW) cells. These results represent the co-contribution of transplanted cells to both functional and morphological reconstitution. (D) GFP$^+$ fibroblasts (FB) were observed near nerve bundles having GFP$^+$ Schwann cells (arrows in D). (E) GFP$^+$ smooth muscle cells were located in conduit blood vessels (arrows in E). (F) Higher magnification of the region outlined in (E) shows sparse contractile filaments (arrows in F) as evidence of vascular smooth muscle cells. (G) GFP$^+$ pericyte-like cells (arrow in G) were also evident in the small capillary. Photographs A, B, and C are from the Sk-34 cell transplantation group, and D-G are from the Sk-DN transplantation group. Scale bars=2 μm.

der. Similar peripheral nerve reconstitution was also reported in the reconstitution of severely damaged skeletal muscle (*10*, *11*) and urethral sphincter (*12*).

With regard to blood vessel reconstitution, transplanted donor-derived cells were mainly incorporated into relatively large blood vessels around the bladder after differentiation into vascular smooth muscles and pericytes. Therefore, blood vessels were not fully reconstituted by transplanted cells in this study, whereas differentiation into blood vessel-related cells, such as pericytes, vascular endothelial cells, and smooth muscle cells, at the same time was observed in the case of severely damaged skeletal muscle reconstitution (*10*, *11*). However, paracrine effects of transplanted cells for surrounding recipient cells are expected to facilitate the present blood vessel reconstitution, as reported for angiogenesis by endothelial progenitor cells (*19*, *20*). These paracrine effects were also supported by the fact that GFP$^+$ fibroblasts were seen around the damaged area (Fig. 5D). Fibroblasts were synthesizing proteins such as cytokines, chemokines, growth factors and extracellular matrix proteins, and participated in the reparative phase of wound healing by producing these proteins (*21*). Thus, paracrine effects by basic fibroblast growth factor, which is one of the factors that induces proliferation of Sk-DN cells, are expected. Importantly, there were no differences in functional recovery between the non–cell-transplanted control 1 and CD45$^+$ cell-transplanted control 2 groups, and there were no GFP$^+$ cells seen after CD45$^+$ cell transplantation. These results clearly indicate that transplantation of muscle-derived CD45$^+$ cells did not enhance the natural functional recovery described above with no cellular engraftment.

In this study, freshly isolated Sk-DN cells were transplanted with freshly isolated Sk-34 cells in the autologous experiment, whereas 5-day cultured Sk-DN cells were used in morphological analysis. This is because it was difficult to perform the transplantation twice for longitudinal analysis in the same individuals in the autologous experiment. Thus, mixed Sk-34+Sk-DN cells were used in single transplantation with the expectation of better results than with the solo transplantation of Sk-34 cells. Sk-DN cells are immature stem cells situated upstream of Sk-34 cells in the same lineage, and they are potentially capable of self-renewal (*22*); thus, the number of Sk-DN cells at initial isolation was extremely small when compared with Sk-34 cells (Sk-DN:Sk-34=1:16–20). As a result of this immaturity, Sk-DN cells have their cell numbers expanded without reducing multipotency, whereas Sk-34 cells are relatively committed stem cells, and their multiple reconstitution capacity is significantly reduced by cell culture. In addition, freshly isolated Sk-DN cells are known to contribute to significant functional and morphological recovery of severely damaged skeletal muscle, whereas the rate of morphological and functional regeneration was lower than in the 6-day cultured Sk-DN cells as they depend on the transplanted cell number (*11*). Thus, similar morphological results were obtained with the present Sk-34 and Sk-DN cell transplantation, as expected from the results of previous reports on cell transplantation into severely damaged skeletal muscle (*10*, *11*); thus, there were no differences in morphological reconstitution capacity between Sk-34 and Sk-DN cells.

Similar cell transplantation of muscle-derived cells isolated, using the preplate technique, in the unilaterally

transected pelvic nerve model in rats has been reported by Kwon et al. (*23*). They also performed functional measurement of intravesical pressures by electrical stimulation of the transected pelvic nerve and obtained significant functional recovery through cross-sectional group comparison analysis at 2 weeks after transplantation. In that report, the recovery period was half of that in the present study, and the morphological contributions of transplanted cells were unclear. However, that report also shows that skeletal muscle-derived cells contribute to the functional recovery of the damaged pelvic nerve.

As a stem cell source of autologous transplantation, muscle-derived stem cells have several advantages because skeletal muscle is the largest organ in the body, comprising ~40% to 50% of total body mass and can be obtained relatively easily and safely. In the case of surgery in lower abdominal organs in humans, if the rectus abdominis muscles were made available for stem cell isolation, we could obtain skeletal muscle from the midline abdominal incision during surgery, and there would be no additional incisions for skeletal muscle sampling. This is advantageous for patients. In addition, autologous transplantation has no risk of immunological rejection, fewer ethical barriers, and markedly lower risk of pathogenic contamination.

However, in stem cell transplantation, there remain concerns over safety aspects such as carcinogenesis. For this aspect, clinical human studies of muscle-derived cell transplantation have recently been performed. Eight women with stress urinary incontinence (SUI) were treated with muscle-derived stem cells obtained from biopsies of the lateral thigh, and improvement in SUI was seen in five of eight women (*24*). Similar autologous transplantation of myoblast/fibroblast mixtures obtained from the left upper arm has also been reported in 123 patients with SUI, using transurethral ultrasound-guided injection. At 1 year after injection, 79% of the women were continent, whereas 21% had substantial or slight improvement (*25*). Two years later, the same group reported outcomes for the same type of autologous transplantation in 18 women with SUI, and 89% of women were cured, with 11% showing improvement (*26*). Importantly, there were no severe postoperative side effects in either experiment. These results clearly indicated that autologous transplantation of muscle-derived cells is basically safe and practical for therapeutic use.

In conclusion, transplantation of skeletal muscle-derived multipotent Sk-34 and Sk-DN stem cells contributed to significant functional recovery of experimental neurogenic bladder dysfunction after reconstitution of damaged BBPP and blood vessels. Therefore, these cells are potentially useful in the treatment of postoperative neurogenic bladder dysfunction after radical hysterectomy for cervical cancer.

REFERENCES

1. Zullo MA, Manci N, Angioli R, et al. Vesical dysfunctions after radical hysterectomy for cervical cancer: A critical review. *Crit Rev Oncol Hematol* 2003; 48: 287.
2. Brooks RA, Wright JD, Powell MA, et al. Long-term assessment of bladder and bowel dysfunction after radical hysterectomy. *Gynecol Oncol* 2009; 114: 75.
3. Abdel-Fattah M, Barrington J, Yousef M, et al. Effect of total abdominal hysterectomy on pelvic floor function. *Obstet Gynecol Surv* 2004; 59: 299.
4. Chen GD, Lin LY, Wang PH, et al. Urinary tract dysfunction after radical hysterectomy for cervical cancer. *Gynecol Oncol* 2002; 85: 292.
5. Todo Y, Kuwabara M, Watari H, et al. Urodynamic study on postsurgical bladder function in cervical cancer treated with systematic nerve-sparing radical hysterectomy. *Int J Gynecol Cancer* 2006; 16: 369.
6. Kato K, Suzuka K, Osaki T, et al. Unilateral or bilateral nerve-sparing radical hysterectomy: A surgical technique to preserve the pelvic autonomic nerves while increasing radicality. *Int J Gynecol Cancer* 2007; 17: 1172.
7. Dursun P, Ayhan A, Kuscu E. Nerve-sparing radical hysterectomy for cervical carcinoma. *Crit Rev Oncol Hematol* 2009; 70: 195.
8. Tamaki T, Akatsuka A, Ando K, et al. Identification of myogenicendothelial progenitor cells in the interstitial spaces of skeletal muscle. *J Cell Biol* 2002; 157: 571.
9. Tamaki T, Akatsuka A, Okada Y, et al. Growth and differentiation potential of main- and side-population cells derived from murine skeletal muscle. *Exp Cell Res* 2003; 291: 83.
10. Tamaki T, Uchiyama Y, Okada Y, et al. Functional recovery of damaged skeletal muscle through synchronized vasculogenesis, myogenesis, and neurogenesis by muscle-derived stem cells. *Circulation* 2005; 112: 2857.
11. Tamaki T, Okada Y, Uchiyama Y, et al. Synchronized reconstitution of muscle fibers, peripheral nerves and blood vessels by murine skeletal muscle-derived CD34(−)/45(−) cells. *Histochem Cell Biol* 2007; 128: 349.
12. Hoshi A, Tamaki T, Tono K, et al. Reconstruction of radical prostatectomy-induced urethral damage using skeletal muscle-derived multipotent stem cells. *Transplantation* 2008; 85: 1617.
13. Okabe M, Ikawa M, Kominami K, et al. "Green mice" as a source of ubiquitous green cells. *FEBS Lett* 1997; 407: 313.
14. Tamaki T, Akatsuka A, Tokunaga M, et al. Characteristics of compensatory hypertrophied muscle in the rat: I. Electron microscopic and immunohistochemical studies. *Anat Rec* 1996; 246: 325.
15. Tamaki T, Uchiyama Y, Okada Y, et al. Multiple stimulations for muscle-nerve-blood vessel unit in compensatory hypertrophied skeletal muscle of rat surgical ablation model. *Histochem Cell Biol* 2009; 132: 59.
16. Tamaki T, Uchiyama Y, Okada Y, et al. Anabolic-androgenic steroid does not enhance compensatory muscle hypertrophy but significantly diminish muscle damages in the rat surgical ablation model. *Histochem Cell Biol* 2009; 132: 71.
17. Tamaki T, Okada Y, Uchiyama Y, et al. Clonal multipotency of skeletal muscle-derived stem cells between mesodermal and ectodermal lineage. *Stem Cells* 2007; 25: 2283.
18. Kuwabara Y, Suzuki M, Hashimoto M, et al. New method to prevent bladder dysfunction after radical hysterectomy for uterine cervical cancer. *J Obstet Gynaecol Res* 2000; 26: 1.
19. Asahara T, Masuda H, Takahashi T, et al. Bone marrow origin of endothelial progenitor cells responsible for postnatal vasculogenesis in physiological and pathological neovascularization. *Circ Res* 1999; 85: 221.
20. Asahara T, Takahashi T, Masuda H, et al. VEGF contributes to postnatal neovascularization by mobilizing bone marrow-derived endothelial progenitor cells. *EMBO J* 1999; 18: 3964.
21. Metz CN. Fibrocytes: A unique cell population implicated in wound healing. *Cell Mol Life Sci* 2003; 60: 1342.
22. Tamaki T, Okada Y, Uchiyama Y, et al. Skeletal muscle-derived CD34+/45− and CD34−/45− stem cells are situated hierarchically upstream of Pax7+ cells. *Stem Cells Dev* 2008; 17: 653.
23. Kwon D, Minnery B, Kim Y, et al. Neurologic recovery and improved detrusor contractility using muscle-derived cells in rat model of unilateral pelvic nerve transection. *Urology* 2005; 65: 1249.
24. Carr LK, Steele D, Steele S, et al. 1-year follow-up of autologous muscle-derived stem cell injection pilot study to treat stress urinary incontinence. *Int Urogynecol J Pelvic Floor Dysfunct* 2008; 19: 881.
25. Mitterberger M, Marksteiner R, Margreiter E, et al. Autologous myoblasts and fibroblasts for female stress incontinence: A 1-year follow-up in 123 patients. *BJU Int* 2007; 100: 1081.
26. Mitterberger M, Pinggera GM, Marksteiner R, et al. Adult stem cell therapy of female stress urinary incontinence. *Eur Urol* 2008; 53: 169.